

A High-Voltage Solid-State Switch Based on Series Connection of IGBTs for PEF Applications

Xiaotian Chen, *Student Member, IEEE*, Lin Yu, Tingting Jiang, Hongping Tian, Kang Huang, and Jianping Wang

Abstract—Pulsed electric field (PEF) technology is a promising nonthermal processing techniques that can be utilized to inactivate microorganisms in liquid food with high-voltage PEF. Herein, a high-voltage solid-state switch consisting of 64 insulated gate bipolar transistors (IGBTs) connected in series was designed and developed for the PEF treatment. Regarding the unbalanced sharing of voltage in series-connected IGBTs, the resistor-capacitor-diode snubber circuit was specifically used and investigated in terms of model of parameters. Furthermore, using gate drivers and optic fiber, the driving circuit and protection circuit were designed and validated. A 50-kV isolation level power supply was built in order to provide 16 independent IGBT stacks with 24 V of power each. The results show that the developed switch works adequately a delay time of 380 ns with 35.8-kV voltage and 44.8-A current capacity. Moreover, the response time of the short-circuit protection is acceptable as well with a reaction time of under 7 μ s. In conclusion, the switch designed for PEF treatment of liquid food performs within set parameters and is ready for pilot-scale processing capability.

Index Terms—High-voltage solid-state switch, insulated gate bipolar transistors (IGBTs), pulsed electric field (PEF), pulsed power, series connection.

I. INTRODUCTION

PULSED electric field (PEF) technology is known as one of the most promising nonthermal processing techniques that can be utilized for the inactivation of microorganisms in liquid food products such as fruit juices and milk [1], [2]. Compared with conventional pasteurization methods using heat to sterilize liquid foods, PEF is able to kill the microorganisms through irreversible electroporation in cell membranes without food heating; therefore, PEF treatment not only inhibits pathogenic and spoilage microorganisms to extend the shelf life but also preserves flavor, aroma, color, and food nutrients [3], [4].

The PEF treatment process involves the application of short-duration (μ s to ms) high-field electric pulses (more than 20 kV/cm) applied to the liquid food flowing between two metal electrodes for microorganism inactivation, which is confined in the chamber [5].

Manuscript received August 29, 2016; revised March 13, 2017 and May 10, 2017; accepted June 4, 2017. Date of publication June 28, 2017; date of current version August 9, 2017. This work was supported by the Chinese National Natural Science Foundation under Grant 31671948. (*Corresponding authors: Kang Huang; Jianping Wang.*)

X. Chen, L. Yu, T. Jiang, H. Tian, and J. Wang are with the College of Biosystems Engineering and Food Science, Zhejiang University, Hangzhou 310058, China (e-mail: jpwang@zju.edu.cn).

K. Huang is with the Department of Food Science and Technology, University of California, Davis, CA 95616, USA (e-mail: kghuang@ucdavis.edu).

Color versions of one or more of the figures in this paper are available online at <http://ieeexplore.ieee.org>.

Digital Object Identifier 10.1109/TPS.2017.2713781

A high-power switch is a primary foundation to generate the high-voltage pulses. For early researches, high-voltage pulses generators with vacuum tubes or spark gaps are used [6]. As the development of semiconductor technology, power semiconductor devices are widely used [7], [8], which have significant advantages compared with a conventional spark-gap switch in repetition rate, lifetime, stability, and compactness. However, the shortcoming of semiconductor devices is their relatively low power capability [9], [10]. For obtaining a proposed solid-state switch for PEF application with adequate voltage, current capability, and repetition rate, it is significant to study technologies of series connection of semiconductor devices.

Metal-oxide-semiconductor field-effect transistors (MOSFETs) and insulated gate bipolar transistors (IGBTs) are the most commonly used semiconductor devices in pulsed-power systems. Compared with MOSFETs which have the advantage of faster switching, IGBTs generally more suitable for high power application. They can handle more power, and are capable of being manufactured at higher voltage and high repetition rate [11], [12]. Therefore, IGBT is competent to develop an adequate power capability switch for PEF applications.

Transient unequal voltage sharing is a major hindrance for a high-voltage solid-state switch based on series-connected IGBTs [13]. The voltage sharing in the transient is decided by many factors such as the device parameter spread and time delay of driver signal [14]. The commonly used signal coupling way including magnetic coupling and optical fiber coupling. Magnetic coupling is a traditional way of signal coupling used to with respect to stability pulse transformer without external gate driver. More power devices used optical fiber to couple signal with the advantage of relatively flexible. The auxiliary circuits used to balance the voltage sharing are divided into load-side voltage balancing technique and gate-side voltage balancing technique. Load-side voltage balancing technique is using the snubber components such as capacitor to minimize the voltage difference while switch is turning ON or turning OFF [15], [16]. And gate-side voltage balancing technique used voltage clamp circuit to limit the voltage of gate and emitter and turning OFF time [17] or different control strategies for the detection of the voltage of gate-emitter or collector-emitter voltage of each IGBT, to form a feedback loop circuit to control IGBT switching, which makes the circuit complex and unreliable [18], [19]. The circuit used in this paper is optical fiber and snubber circuit to mitigate the unequal sharing voltage in the IGBT series topology.

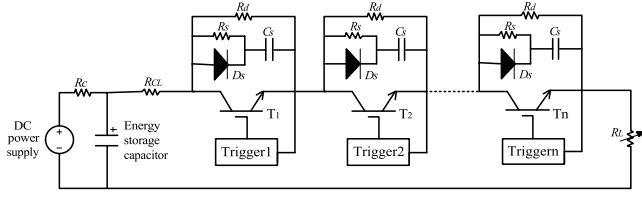


Fig. 1. Series connection of IGBTs with RCD snubber circuits.

In this paper, a repetitive high-power solid-state switch for liquid food PEF treatment was designed and implemented using series-connected discrete IGBTs. A mathematical model of resistor–capacitor–diode (RCD) snubber circuit for active voltage balance was developed to optimize parameters. Combined with the snubber circuit, the IGBT gate driving circuit was designed based on digital signal processor (DSP) and optical fiber, which was overcoming the problem of unbalance voltage sharing. Furthermore, a protection circuit was developed to shut down the IGBT stacks when the load was shorted. Finally, the designed switch was applied to PEF processing system to test its long-term stability.

II. EXPERIMENTAL SETUP

First, we introduce the process of RCD snubber circuit modeling, and then present the design of IGBT stacks and isolated high-voltage power supply in detail.

A. Model of RCD Snubber Circuit Parameters

Fig. 1 shows a schematic model of the series-connected IGBTs with RCD snubber circuits. The dynamic clamping circuit comprises a resistor (R_s), capacitor (C_s), and diode (D_s). This circuit slows down the dv/dt of the turn-OFF process to suppress the transient overvoltage with the parallel capacitor C_s . D_s provides a low-impedance path when C_s is charged, and R_s limits the current when C_s discharges in the switching transient.

C_s is used to slow down the steep fluctuation of the voltage. In this manner, the voltages tend to rise slowly, which can prevent surges. However, selecting the value of C_s is critical. A large value of C_s will extend the switching time, whereas a small value cannot slow down the steep change of the voltage. Likewise, when R_s is excessively small, a large current will occur, which may damage the devices. By contrast, a large value of R_s can reduce the speed of C_s discharging.

The differences of the driving signal transmission time and switch characteristics of IGBTs lead to the asynchronization in IGBTs switching. If we take the IGBT first turning ON as a reference, there are $n-1$ units time of switching delay existing in the circuit of n series-connected IGBTs. Assuming x IGBTs are delayed to turn ON while $n-x$ IGBTs have been turned ON, then x snubber capacitors C_s will be connected in series, and the equivalent capacitance is C_s/x . R_s is short circuited by D_s , and the series-connected snubber capacitors are charged through load resistance R_L with the RC time constant of $C_s R_L/x$. When switching delay occurs, the rising speeds of the voltage of delayed IGBTs are unequal. The increased voltage ΔU_x of IGBTs during x units time of switching delay (t_x)

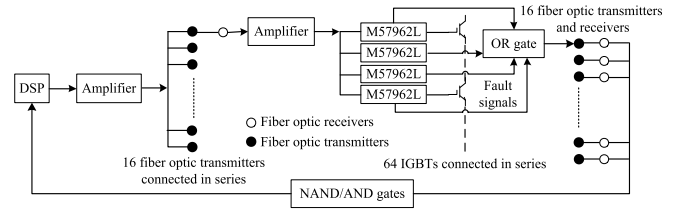


Fig. 2. Design principle of the IGBT stack.

can be calculated as follows:

$$\Delta U_x = \frac{(U_{DC} - U_F - \dots - \Delta U_{x-1})}{n-x} \cdot \left[1 - e^{-\frac{(n-x)t_x}{R_L \cdot C_s}} \right] \quad (1)$$

where U_{DC} represents the dc power supply voltage and U_F represents the theoretic voltage of each IGBT in OFF state, which indicates that U_F is equal to U_{DC}/n .

The increased voltage ΔU of the last IGBT to be turned ON can be written as

$$\begin{aligned} \Delta U_x = & \frac{(U_{DC} - U_F)}{n-1} \cdot \left[1 - e^{-\frac{(n-1)t_1}{R_L \cdot C_s}} \right] + \frac{(U_{DC} - U_F - \Delta U_1)}{n-2} \\ & \cdot \left[1 - e^{-\frac{(n-2)t_2}{R_L \cdot C_s}} \right] \\ & + \dots + \Delta U_x + \dots + (U_{DC} - U_F - \dots - \Delta U_{n-2}) \\ & \cdot \left(1 - e^{-\frac{t_{n-1}}{R_L \cdot C_s}} \right). \end{aligned} \quad (2)$$

Equation (2) indicates that if the voltage U_L of the IGBT, that is, last turned ON does not exceed the blocking voltage $U_{CE(max)}$ of IGBT, then other $(n-1)$ IGBTs are working under the voltage of $U_{CE(max)}$, which means

$$\Delta U = U_L - U_F \leq U_{CE(max)} - U_F. \quad (3)$$

According to (1), the equivalent capacitance will decrease as more IGBTs are turned ON, whereas the increased voltage will equally fall onto other IGBTs that remain turned OFF. Thus, the rising speed of ΔU_x will be higher as more IGBTs are turned ON. Assuming the total delay time of the IGBT that is last to be turned ON as Δt , and ΔU is increased as fast as the end of the polynomial of the right side of (3). When $(n-1)$ IGBTs are turned ON simultaneously, only one IGBT will be delayed to turn ON, and then ΔU will be the largest compared with other situations wherein more than one IGBT are delayed to turn ON. Thus, (3) can be modified as follows:

$$\Delta U < (U_{DC} - U_F) \cdot (1 - e^{-\Delta t / C_s \cdot R_L}) \leq U_{CE(max)} - U_F. \quad (4)$$

Then, the value of C_s can then be calculated according to (4) and expressed in the following equation:

$$C_s \geq -\frac{\Delta t}{R_L \cdot \ln \frac{n - U_{CE(max)}/U_F}{n-1}}. \quad (5)$$

Fig. 2 indicates that while IGBT turns ON, the current of its collector is equal to the sum of the load current I_L and discharge current (I_{CS}) of C_s , which can be written as follows:

$$\begin{aligned} I_{CS} + I_L = & (\Delta U + U_F)/R_s + I_L \leq U_{CEmax}/R_s \\ & + I_{L(max)} \leq I_{C(max)} \end{aligned} \quad (6)$$

where $I_{c(\max)}$ means the largest current that the IGBT can be withstood. While the IGBT turns ON, C_S begins to discharge. If the time that the IGBT keeps turning ON is τ , the voltage of C_S should decrease to U_F during the time $\tau - \Delta t$ to keep the voltage of IGBT below U_F . This relation can be expressed as follows:

$$\begin{aligned} \Delta U_{(\tau-\Delta t)} &= (\Delta U + U_F) \cdot e^{-\frac{\tau-\Delta t}{C_S} \cdot R_L} \\ &\leq U_{CE(\max)} \cdot e^{-(\tau-\Delta t)/C_S \cdot R_L} \leq U_F. \end{aligned} \quad (7)$$

Assuming the power loss of a single R_S is P_{RS} , then P_{RS} can be written as follows:

$$P_{RS} = f \cdot C_S \cdot (\Delta U + U_F)^2 \cdot f/2 \leq f \cdot C_S \cdot U_{CE(\max)}^2/2. \quad (8)$$

We define k as the ratio of $U_{ce(\max)}$ and U_F , and the mathematical model of the RCD snubber can be written as follows:

$$\begin{cases} C_S \geq -\frac{\Delta t}{R_L [\ln(n-k) - \ln(n-1)]}, & U_{BR(C)} > U_{CE(\max)} \\ \frac{U_{CE(\max)}}{I_{C(\max)} - I_{L(\max)}} \leq R_S \leq \frac{\tau - \Delta t}{C_S \ln k}, & P_{RS} \geq f C_S U_{CE(\max)}^2/2 \\ U_{BR(D)} > U_{CE(\max)}, & I_{F(D)} > U_{DC}/R_l \end{cases} \quad (9)$$

where $U_{BR(C)}$ and $U_{CE(\max)}$ are the breakdown voltage of C_S and D_S , respectively. $I_{F(D)}$ is the maximum current that the diode can be withstood.

B. Designed of IGBT Stacks

To provide a 40-kV voltage for PEF treatment, 64 series-connected IGBTs are used in this experiment. Thus, the voltage for each IGBT in this paper is 625 V. IGBT stacks are composed of IGBTs (Infineon, IGW60T120) rated to 1200-V and a 60-A continuous current. A non-punch through-type IGBT is regarded to be nearly ideal for series stack assemblies. According to its datasheet, the IGBT can theoretically handle a 150-A collector current.

Fig. 2 shows the scheme of IGBT stacks. A DSP (TI, TMS320F28335) is used to send out the pulswidth modulation (PWM) signals, in which the width and frequency of pulse can be adjusted in succession according to different pasteurization requirements. These signals are amplified up to drive 16 fiber-optic transmitters (Avago, HFBR-1414), all of which are connected in series. A total of 16 driving signals are transmitted through fiber optics to corresponding amplifiers, and each amplifier can operate four series-connected gate drivers (Mitsubishi, M57962L). An IGBT stack is mainly composed of four IGBTs and IGBT drivers, and the M57962L has built-in circuits that will protect the IGBT from short circuit by detecting desaturation. When a short circuit occurs, a high current flows through the IGBT, which will cause its collector to emit voltage into the higher level than a normal operation. When the hybrid driver detects this condition, the driver quickly turns the IGBT OFF, and sends out fault signal. Fig. 2 indicates that four M57962Ls corresponding to one amplifier will produce four fault signals, which are placed into one OR gate and then transmitted through another fiber optics into the NAND/AND gate. The feedback signals will be

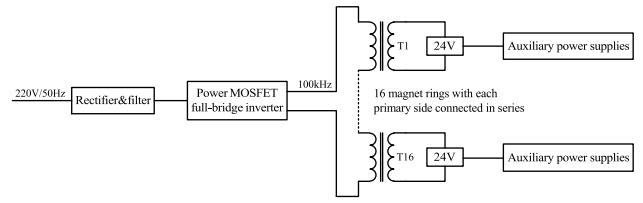


Fig. 3. Diagram of the isolated high-voltage power supply system.

imported into DSP, which then stop producing PWM signals immediately to ensure the safety of IGBTs.

Given that the number of IGBTs used for series connection is quite large, one of the difficulties we had to solve is how to achieve synchronous switching of all 64 IGBTs. After finishing the trigger unit according to Fig. 2, the time differences in turning ON and OFF between IGBTs are tested. The experimental results show that the delay time between two neighboring IGBTs is approximately 20–25 ns, as controlled by the same amplifier. The largest delay time among all IGBTs ranges from 90 to 140 ns. The turning ON/OFF time difference of IGBTs is affected by both signal transmission time and the characteristics of each IGBT. The former can be improved by the trigger unit, whereas the latter cannot be controlled manually. Thus, we believe that the 140-ns time delay between 64 series-connected IGBTs is acceptable.

The largest pulsed collector current of IGBTs is set to be 100 A, which is less than the theoretical collector current of 150 A. Higher frequency pulses usually produce more heat, which causes a considerable temperature rise. The frequency of pulses is not extremely high for PEF treatment, so the frequency used in the proposed system is set to be less than 1000 Hz. According to (3), the calculating value of C_S is 0.02 μ F. Actually, the value of C_S is set to be 0.033 μ F/2000 V for safety concerns. The value of R_S is approximately 24 Ω /24 W to 110 Ω /24 W, and two 33 Ω /30 W power resistors connected in series are used as the snubber resistor. Two fast-switching diodes (Infineon, IDB30E120) rated to 1200-V and 50-A continuous current connects in parallel are used in each RCD snubber. The maximum repetitive forward current of IDB30E120 is 76.5 A based on the Infineon datasheet. Thus, the rated current of two parallel-connected diodes is 153 A, which is larger than the operating current of 100 A.

C. Design of Isolated High-Voltage Power Supply

As shown in Fig. 2, all devices including the amplifiers and drivers necessitate auxiliary power supplies. IGBT stacks are operated at a voltage of 40 kV. Thus, all auxiliary power supplies have a 40-kV potential. The isolation voltage of all auxiliary power supplies should be greater than 40 kV. The 64 IGBTs are divided into 16 groups, and the average voltage of each group is 2500 V. In each group, the potential difference between the first and fourth IGBTs is 1875 V. Thus, the isolation voltage of the auxiliary power supplies must be greater than 1875 V for each group. Fig. 3 shows the diagram of the isolation high-voltage power supply system.



Fig. 4. 50-kV isolation auxiliary power supply for IGBT stacks.

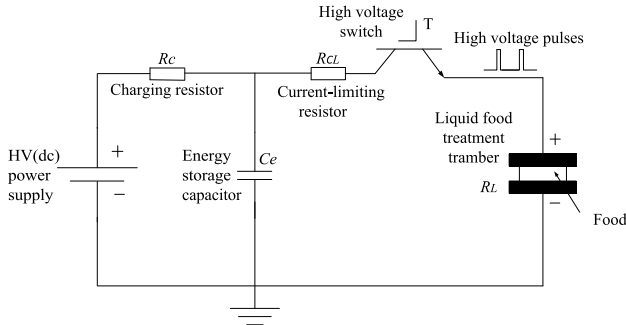


Fig. 5. Schematic circuit of testing system.

To obtain power supplies with different voltages, a 50-kV isolated circuit to obtain 16 completely independent 24-V supplies is designed, which will be used for 16 IGBT stacks. And in the IGBT stack, each 24-V supply can be converted to 15 and -10 V for M57962L, and 5 V for fiber-optic receivers.

As shown in Fig. 3, after the 220 V/50 Hz ac is converted to 310-V dc, the power MOSFET full-bridge inverter transforms the dc into a square wave pulse with a frequency of 100 kHz. Then, this square wave pulse will be imported to 16 transformers, the primary sides of which are all connected in a series by a silicone rubber insulated wire with a 50-kV isolated voltage. Given the high-frequency pulses, an Fe-based amorphous core is used as the material for the transformer. Fig. 4 shows a photograph of the 16 independent 24-V power supplies with a 50-kV isolation voltage.

III. TEST RESULTS AND ANALYSIS

Tests are carried out according to the schematic, as shown in Fig. 5. The PEF treatment system for test consists of a high-voltage power, a charging resistor, an energy storage capacitor, a high-voltage switch, and a food treatment chamber. Energy storage capacitor C_e is charged through resistor R_c by high-voltage dc power supply (WWL-LDG, Shuanghong Electronics, Jiangsu, China), whose maximum output voltage is 50 kV and rated output current is 5 mA. When the high-voltage solid-state switch controls capacitor C_e charging and discharging to deliver energy into the treatment chamber continuously. The 200- Ω current-limiting resistor R_{CL} plays a role to prevent excessive current.

The co-field treatment chamber is a widely used in PEF processing system. In our experiments, the load shown

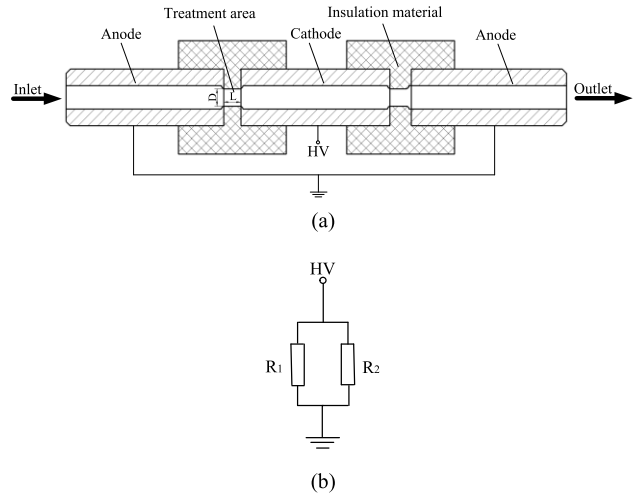


Fig. 6. (a) Co-field treatment chamber used in experiment and (b) its equivalent circuit.

TABLE I
MAJOR PARAMETERS OF INSTRUMENTS USED IN TEST

Instrument	Bandwidth	Rise time	Range
Voltage probe	75MHz	≤ 4.67 ns	1.5kV to 20 kV DC/ 40 kV peak
Current probe	50MHz	≤ 7 ns	50A DC

in Fig. 6(a) is used, whose equivalent circuit is given in Fig. 6(b).

Here, the two treatment areas are regarded as two parallel-connected resistors, which are function of electrical conductivity of the liquid. As shown in Fig. 6(b), D and L represent the diameter and length of the cylindrical chamber area, respectively. Thus, the total resistance in the discharge loop is expressed in the following equation:

$$R_T = R_{CL} + R_L = R_{CL} + \frac{2L}{\sigma \pi D^2} \quad (10)$$

where σ is the electrical conductivity of the liquid flowing through the chambers, and R_T can be changed easily by changing σ . In this paper, we intend to determine whether the IGBT stack can safely work under different test conditions, such as high-voltage and short-circuit conditions. Thus, the sterilization effect is not considered in this paper. The sodium chloride (NaCl) solution with different electrical conductivities is chosen as the treatment medium. During the test, we select oscilloscope (TDS2002C, Tektronix, TX, USA) for measurement, whose maximum sample rate is 1 GS/s and bandwidth is 70 MHz. A high-voltage probe (P6015A, Tektronix, TX, USA) and a current probe (TCP305, Tektronix, TX, USA) are used to capture the voltage and current waveforms, respectively. Table I shows the major parameters of these two instruments.

A. High-Voltage Test

A photograph of the assembled IGBT stack is shown in Fig. 7. A total of printed circuit boards (PCBs) that corresponds to 16 groups of series-connected IGBTs are included



Fig. 7. Assembled IGBT stacks which are composed of 64 series-connected IGBTs.

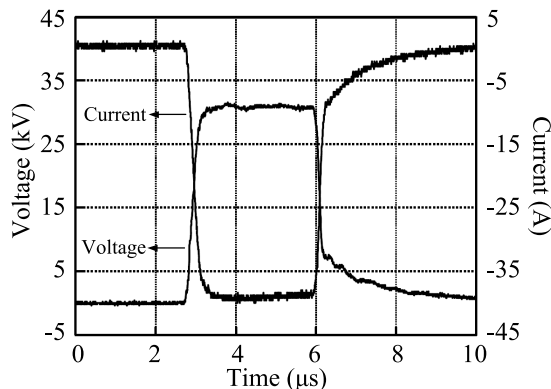


Fig. 8. Waveforms of voltage and current of treatment chambers. The dc power supply is 40 kV, the pulse with is $3 \mu\text{s}$, and the maximum voltage and maximum current of chambers are 31.6 kV and 40 A, respectively.

in the photograph. Each PCB has a signal input and a fault signal output, all of which are transmitted through fiber optics.

During measurements, the PCBs are added one by one, and 2500 V of voltage is added at each instance. The voltage of the chambers is measured, as well as the circuit current. The measurement result is shown in Fig. 8, when the high-voltage dc power supply is set to be 40 kV. The falling edge represents the turn-OFF procedure of series-connected IGBTs. As shown in Fig. 8, in process of turning OFF, the voltage falls fast at the beginning, and then slows down. Once the IGBTs are turned OFF, all the snubber capacitors become series-connected and charge, which are considered as a short circuit. It deserves to be specially noted that the voltage of the capacitor cannot change immediately when the IGBTs are turned OFF. However, the voltage of capacitors approaches zero when in the state of turning ON. Therefore, the voltage of IGBT falls rapidly in the beginning of turning OFF, until the snubber capacitor starts to work which will slow down the rate of voltage falling.

B. Short-Circuit Protection Test

Because of ohmic heating, numerous bubbles unavoidably appear in liquids during the continuous PEF processing, which may cause breakdown in the treatment chamber and short circuit under the high voltage. The degassing method is often used on liquids before PEF treatment to decrease the possibility of breakdown [1]. However, this method cannot

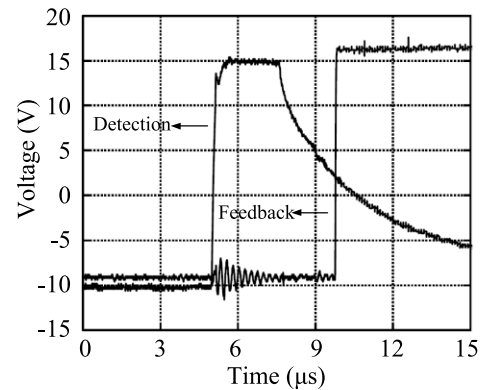


Fig. 9. Detection signal of M57962L and overcurrent feedback signal while short circuit occurs.

completely prevent short circuit happening in treatment chambers. Therefore, short circuit protection is indispensable for a continuous PEF treatment system.

While the driving voltage is 15 V, the short-circuit withstand time of IGBT is only $10 \mu\text{s}$ and the allowed time between short time should be more than 1 s based on the datasheet of IGBT. Although M57962L can perform a soft shutdown of the IGBT when short circuit occurs, the next pulse will drive IGBTs again, which can damage all of series-connected IGBTs directly. Therefore, the whole IGBT stack should be turned OFF before the DSP sends out the next drive signal. The delay time described in this paper is for the series-connected IGBTs, not for single IGBT. It is impossible that each IGBT in the series-connected circuit has absolutely the same rate of turn-ON time, which depends on these three factors: individual characteristic of IGBT, transferring time of drive signal and drive voltage of IGBT, so the delay time of the series-connected IGBTs is determined. Fig. 9 shows the measurement result of the drive signal from M57962L and the feedback signal input to DSP when short circuit is detected.

The overcurrent feedback signal is produced by M57962L, which has the function of detecting overcurrent and short circuit by monitoring V_{ce} of IGBTs. As shown in Fig. 9, when an overcurrent or a short circuit occurs, a feedback signal is sent to DSP after the occurrence of $6 \mu\text{s}$. As the DSP responds in a few nanoseconds, the response time of short circuit protection can be regarded as $7 \mu\text{s}$ totally, which is less than the short circuit withstand time ($10 \mu\text{s}$) of these IGBTs. Thus, if the protection circuit could capture this signal and respond in time, the whole system will be shut down immediately to prevent the switch from being damaged. However, due to the existence of the detection time, the gate driver cannot send out fault signals in time while the pulsewidth is less than $2.5 \mu\text{s}$ in the case of overcurrent or short circuit. To avoid such damage, the pulsewidth of this pulse generator is set to be no less than $2.5 \mu\text{s}$.

C. Model of RCD Snubber Parameters Test

With the aim of capturing the current waveform of the treatment chambers, the equivalent resistance of the treatment chamber is set to be 800Ω by changing the electrical conductivity of NaCl solution, and the total resistance R_T in the loop

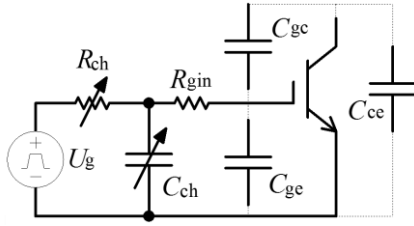


Fig. 10. Method of changing gate resistor R_g and input capacitor C_{ies} .

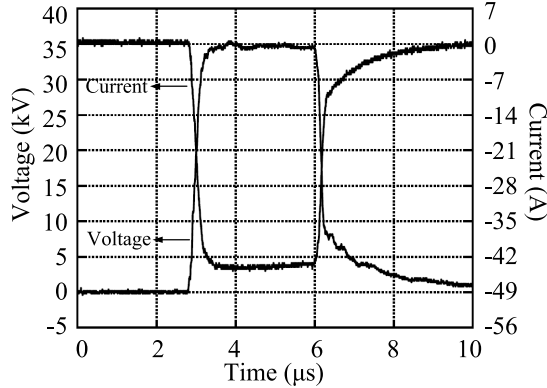


Fig. 11. Measured voltage and current of treatment chambers while the dc power supply is 45 kV. The tested maximum voltage and maximum current are 35.8 kV and 44.8 A, respectively.

is 1000 Ω . However, this value is quite larger than 400 Ω that we used to calculate the C_s . Also, 0.033 μF is larger than the theoretical value (0.02 μF). We want to determine if (9) still stands when C_s is minimized.

The 50-kV isolation voltage and the maximum voltage (50 kV) of the dc power supply we used in our previous tests determine the value that we will use in this test. The average voltage of each IGBT is then set at 700 V; thus, IGBT stacks can be efficient under the voltage of 44.8 kV. Based on (9), Δt is 38 ns. The turning ON of the IGBT is regarded as the charging effect of IGBT's input capacitor (C_{ies}), and the gate resistor is the charging resistor. The turn-ON delay time (t_d) can be deduced as shown in the following:

$$t_d = R_g \cdot C_{ies} \cdot \ln \frac{V_{g1} - V_{g2}}{V_{g1} - V_T} \quad (11)$$

where V_{g1} and V_{g2} are turn-ON and turn-OFF voltages of gate-emitter voltage (V_{ge}) supplied by the driver, the value of which are +15 and -10 V, respectively. V_T represents the gate-emitter threshold voltage of IGBT, which is 5.8 V based on the datasheet. If we change R_g or C_{ies} , the turn-ON delay time will also be changed. To obtain 380-ns delay time, the value of both R_g and C_{ies} should be changed using an adjustable resistor (R_{ch}) rates at 51 Ω and an adjustable capacitor (C_{ch}) rates at 18 nF. The method is shown in Fig. 10, in which the total R_g is the sum of R_{ch} and R_{gin} . The total C_{ies} is the sum of C_{ch} , C_{gc} , and C_{ge} . R_{gin} , C_{gc} , and C_{ge} , which are interparameters of IGW60T120 that can be obtained from its datasheet.

The validation test of C_s is conducted at the delay time of 380 ns. During the test, the IGBT stack works efficiently.

Fig. 11 shows the measurement result of the voltage and the current of treatment chambers. While the high-voltage dc power supply is working at 45 kV, the voltage is 35.8 kV, and the current is 44.8 A. The result of tests demonstrates that C_s works at its minimum value, and the method of circulating C_s is practicable. Output peak voltage is about 80% of the dc link voltage, which is caused by the use of the current-limiting resistor. The behavior of reduced falling edge is similar to that shown in Fig. 8, both of which are caused by the effect of snubber capacitor.

IV. CONCLUSION

In this paper, a high-voltage solid-state switch based on 64 series-connected IGBTs for PEF processing system has been developed. To ensure an equal sharing of voltage occurring in IGBT series topology, a detailed mathematical model of RCD snubber circuit for active voltage balance is developed, which is demonstrated by further tests. Based on DSP and IGBT driver, the driving and short-circuit protection circuit is designed and implemented. Optical fibers are used to ensure the synchronization of signal and potential isolation. The maximum turn-ON time difference among all of 64 IGBTs is 120 ns. Based on 16 Fe-based amorphous core, the 50-kV isolation power system is established to provide 16 independent 24-V power supplies for 16 groups of series-connected IGBTs.

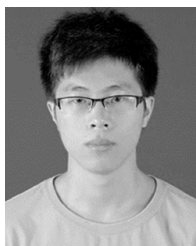
The application of designed switch in the high-voltage pulse generator for PEF processing suggests that the pulse generator could produce high-voltage square wave pulses with steep edge stably. Furthermore, results show that the developed switch performs adequately with a time delay of 380 ns, drawing a total of 35.8 kV of voltage and 44.8 A of current and its protection circuit with a response time of under 7 μs is able to sufficiently prevent possible damage to the switch. However, due to the current detection time of 2.5 μs , the protection circuit is effective only for pulses with larger than 2.5- μs duration.

To improve the stability of the high-voltage switch and processing capability of PEF treatment system, the further study of IGBTs in a parallel topology would be needed.

REFERENCES

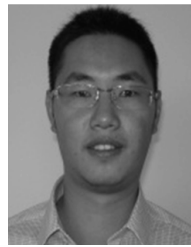
- [1] H. W. Yeom, C. B. Streaker, Q. H. Zhang, and D. B. Min, "Effects of pulsed electric fields on the quality of orange juice and comparison with heat pasteurization," *J. Agricult. Food Chem.*, vol. 48, no. 10, pp. 4597–4605, Oct. 2000.
- [2] J. Chen *et al.*, "Influence of pulse rise time on the inactivation of staphylococcus aureus by pulsed electric fields," *IEEE Trans. Plasma Sci.*, vol. 38, no. 8, pp. 1935–1941, Aug. 2010.
- [3] S. Min, G. A. Evrendilek, and H. Q. Zhang, "Pulsed electric fields: Processing system, microbial and enzyme inhibition, and shelf life extension of foods," *IEEE Trans. Plasma Sci.*, vol. 35, no. 1, pp. 59–73, Feb. 2007.
- [4] R. Zhang, L. Cheng, L. Wang, and Z. Guan, "Inactivation effects of PEF on horseradish peroxidase (HRP) and pectinesterase (PE)," *IEEE Trans. Plasma Sci.*, vol. 34, no. 6, pp. 2630–2636, Dec. 2006.
- [5] S. R. Alkhafaji and M. Farid, "An investigation on pulsed electric fields technology using new treatment chamber design," *Innov. Food Sci. Emerg. Technol.*, vol. 8, no. 2, pp. 205–212, Jun. 2007.
- [6] E. J. M. van Heesch *et al.*, "A fast pulsed power source applied to treatment of conducting liquids and air," *IEEE Trans. Plasma Sci.*, vol. 28, no. 1, pp. 137–143, Feb. 2000.

- [7] M. Gaudreau, T. Hawkey, J. Petry, and M. Kempkes, "Solid-state power systems for pulsed electric field (PEF) processing," in *Proc. IEEE Pulsed Power Conf.*, Monterey, CA, USA, Jun. 2005, pp. 1278–1281.
- [8] H. A. Prins, R. H. S. H. Beurskens, Y. L. M. Creyghton, N. Dutreus, S. W. H. de Haan, and B. Roodenburg, "Solid state pulsed power source for pulsed electric field and plasma treatment of food products," in *Pulsed Power Plasma Sci. Dig. Tech. Paper*, Las Vegas, NV, USA, Jun. 2001, pp. 1294–1297.
- [9] W. H. Jiang, "Fast high voltage switching using stacked MOSFETs," *IEEE Trans. Dielectr. Electr. Insul.*, vol. 14, no. 4, pp. 947–950, Aug. 2007.
- [10] W. Jiang *et al.*, "Compact solid-state switched pulsed power and its applications," *Proc. IEEE*, vol. 92, no. 7, pp. 1180–1196, Jul. 2004.
- [11] E. G. Cook, "Review of solid-state modulators," in *Proc. 4th Int. Conf. Elect. Eng.*, Monterey, CA, USA, Aug. 2000, pp. 663–667.
- [12] S. Castagno, R. D. Curry, and E. Loree, "Analysis and comparison of a fast turn-on series IGBT stack and high-voltage-rated commercial IGBTs," *IEEE Trans. Plasma Sci.*, vol. 34, no. 5, pp. 1692–1696, Oct. 2006.
- [13] N. Y. A. Shammas, R. Withanage, and D. Chamund, "Review of series and parallel connection of IGBTs," *IEE Proc.-Circuits, Devices Syst.*, vol. 153, no. 1, pp. 34–39, Feb. 2006.
- [14] T. Van Nguyen, P.-O. Jeannin, E. Vagnon, D. Frey, and J.-C. Crebier, "Series connection of IGBTs with self-powering technique and 3-D topology," *IEEE Trans. Ind. Appl.*, vol. 47, no. 4, pp. 1844–1852, Jul./Aug. 2011.
- [15] M. Zarghani, S. Mohsenzade, and S. Kaboli, "A fast and series-stacked IGBT switch with balanced voltage sharing for pulsed power applications," *IEEE Trans. Plasma Sci.*, vol. 44, no. 10, pp. 2013–2021, Oct. 2016.
- [16] T. C. Lim, B. W. Williams, and S. J. Finney, "Active snubber energy recovery circuit for series-connected IGBTs," *IEEE Trans. Power Electron.*, vol. 26, no. 7, pp. 1879–1889, Jul. 2011.
- [17] F. Bauer, L. Meysenc, and A. Piazzesi, "Suitability and optimization of high-voltage IGBTs for series connection with active voltage clamping," *IEEE Trans. Power Electron.*, vol. 20, no. 6, pp. 1244–1253, Nov. 2005.
- [18] S. Ji, T. Lu, Z. Zhao, H. Yu, and L. Yuan, "Series-connected HV-IGBTs using active voltage balancing control with status feedback circuit," *IEEE Trans. Power Electron.*, vol. 30, no. 8, pp. 4165–4174, Aug. 2015.
- [19] R. Withanage and N. Shammas, "Series connection of insulated gate bipolar transistors (IGBTs)," *IEEE Trans. Power Electron.*, vol. 27, no. 4, pp. 2204–2212, Apr. 2012.



Xiaotian Chen (S'17) was born in Hangzhou, Zhejiang, China. He received the B.S. degree in mechanical engineering from Zhejiang Science and Technology University, Hangzhou, in 2011. He has been pursuing the Ph.D. degree in agricultural mechanization engineering with Zhejiang University, Hangzhou, since 2015.

His current research interests include pulsed-power technology and its applications on food processing.



Lin Yu was born in Hangzhou, Zhejiang, China. He received the Ph.D. degree in agricultural electrification and automation from the College of Biosystems Engineering and Food Science, Zhejiang University, Hangzhou, in 2012.

His current research interests include pulsed-power technology and its applications, and the modeling and simulation of power semiconductors.



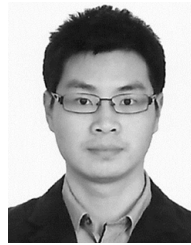
Tingting Jiang was born in Fujian, China. She received the M.D. degree in agricultural electrification and automation from the College of Biosystems Engineering and Food Science, Zhejiang University, Hangzhou, Zhejiang, China, in 2014.

Her current research interests include the design of pulsed electric field system for liquid food sterilization.



Hongping Tian was born in Hangzhou, Zhejiang, China. She received the M.D. degree from Zhejiang University, Hangzhou, in 2003.

She is currently a Lecturer with the Party Working Committee of Huajiachi Campus, Zhejiang University. She is involved in the research of processing of agricultural products.



Kang Huang was born in Hangzhou, Zhejiang, China. He received the Ph.D. degree from Zhejiang University, Hangzhou, in 2014.

He is currently a Post-Doctoral Scholar with the Department of Food Science and Technology, University of California, Davis, CA, USA. His current research interests include the food processing and food packaging.



Jianping Wang was born in Harbin, Heilongjiang, China. He received the Ph.D. degree from Northeast Agricultural University, Harbin.

He is currently a Professor with the Department of Biosystems Engineering, College of Biosystems Engineering and Food Science, Zhejiang University, Hangzhou, China. He is involved in the research of intelligent agricultural equipment and pulsed electric field technology.